HUMAN GENE THERAPY 23:56–69 (January 2012)

DOI: 10.1089/hum.2011.054

Efficient Generation of A9 Midbrain Dopaminergic Neurons by Lentiviral Delivery of LMX1A in Human Embryonic Stem Cells and Induced Pluripotent Stem Cells

A. Sánchez-Danés,[1,2,*] A. Consiglio,[1,2,3,*] Y. Richaud,[4,5] I. Rodríguez-Pizà,[2] B. Dehay,[6,7,8] M. Edel,[9,†] J. Bové,[4,6] M. Memo,[3] M. Vila,[6,7,10] A. Raya,[4,5,10] and J.C. Izpisua Belmonte[2,11]

Abstract

Human embryonic stem cells (hESC) and induced pluripotent stem cells (iPSC) offer great hope for *in vitro* modeling of Parkinson's disease (PD), as well as for designing cell-replacement therapies. To realize these opportunities, there is an urgent need to develop efficient protocols for the directed differentiation of hESC/iPSC into dopamine (DA) neurons with the specific characteristics of the cell population lost to PD, *i.e.*, A9-subtype ventral midbrain DA neurons. Here we use lentiviral vectors to drive the expression of *LMX1A*, which encodes a transcription factor critical for ventral midbrain identity, specifically in neural progenitor cells. We show that clonal lines of hESC engineered to contain one or two copies of this lentiviral vector retain long-term self-renewing ability and pluripotent differentiation capacity. Greater than 60% of all neurons generated from LMX1A-engineered hESC were ventral midbrain DA neurons of the A9 subtype, compared with ~10% in green fluorescent protein–engineered controls, as judged by specific marker expression and functional analyses. Moreover, DA neuron precursors differentiated from LMX1A-engineered hESC were able to survive and differentiate when grafted into the brain of adult mice. Finally, we provide evidence that *LMX1A* overexpression similarly increases the yield of DA neuron differentiation from human iPSC. Taken together, our data show that stable genetic engineering of hESC/iPSC with lentiviral vectors driving controlled expression of LMX1A is an efficient way to generate enriched populations of human A9-subtype ventral midbrain DA neurons, which should prove useful for modeling PD and may be helpful for designing future cell-replacement strategies.

Introduction

Parkinson's disease (PD) is an incurable, chronically progressive condition characterized by the continuing degeneration of dopamine (DA) neurons projecting from the midbrain substantia nigra to the basal ganglia striatum (Marsden, 1990). Current symptomatic therapies, consisting primarily of pharmacological DA replacement, compensate the movement deficit efficiently over a period of several years, but are ineffective in alleviating the loss of autonomic and cognitive abilities. Moreover, current treatments are met with late complications, which might be due, at least partially, to neurotoxicity of the drugs.

The localized loss of a specialized neuronal cell population, paired with the urgent need for long-term treatment options, makes cell replacement therapy a promising

[1]Institute of Biomedicine of the University of Barcelona (IBUB), Barcelona, Spain.
[2]Center for Regenerative Medicine in Barcelona, Barcelona, Spain.
[3]Department of Biomedical Science and Biotechnology, University of Brescia, Brescia, Italy.
[4]Control of Stem Cell Potency Group, Institute for Bioengineering of Catalonia (IBEC), Barcelona, Spain.
[5]Networking Center of Biomedical Research in Bioengineering, Biomaterials and Nanomedicine (CIBER-BBN), Barcelona, Spain.
[6]Neurodegenerative Diseases Research Group, Vall d'Hebron Research Institute, Barcelona, Spain.
[7]Networking Center of Biomedical Research on Neurodegenerative Diseases (CIBERNED), Barcelona, Spain.
[8]Institut des Maladies Neurodégénératives, Université de Bordeaux and CNRS, UMR 5293, F-33000 Bordeaux, France.
[9]Research Institute of Hospital Vall d'Hebron and Banc de Sang i Teixits, Advanced Cell Therapies and Immunology, Barcelona, Spain.
[10]Catalan Institution for Research and Advanced Studies (ICREA), Barcelona, Spain.
[11]Gene Expression Laboratory, Salk Institute for Biological Studies, La Jolla, CA.
*A.S.-D. and A.C. contributed equally to this work.
[†]Affiliated as Visiting Research Fellow at the Victor Chang Cardiac Research Institute, Sydney, Australia.

approach to treat PD. Clinical trials involving grafting of embryonic ventral mesencephalic tissue in PD patients have provided proof-of-concept for the feasibility of cell therapy in this disease (Lindvall and Björklund, 2004). However, this approach is not widely applicable owing to the limited supply of such tissues and to ethical concerns.

Human pluripotent stem cells, such as human embryonic stem cells (hESC) (Thomson *et al.*, 1998), have great potential regarding their therapeutic use for PD patients (Lee *et al.*, 2000; Ying *et al.*, 2003; Nat *et al.*, 2007; Morizane *et al.*, 2008). More recently, the generation of induced pluripotent stem cells (iPSC) by ectopic expression of a defined set of factors (Takahashi *et al.*, 2007; Yu *et al.*, 2007; Aasen *et al.*, 2008; Lowry *et al.*, 2008; Park *et al.*, 2008b) has enabled the derivation of patient-specific pluripotent cells, providing valuable experimental platforms to model human disease (Dimos *et al.*, 2008; Park *et al.*, 2008a; Ebert *et al.*, 2009; Soldner *et al.*, 2009; Agarwal *et al.*, 2010) and opening the possibility of implementing patient-matched cell-therapy applications (Hanna *et al.*, 2007; Wernig *et al.*, 2008; Raya *et al.*, 2009). In addition, the possibility of genetically engineering human pluripotent stem cells to express potentially therapeutic molecules or to manipulate their differentiation toward a specific phenotype, which, for example, could be used to increase survival, differentiation, migration, and function of their progeny, creates new opportunities for the development of restorative treatment for PD patients.

The use of hESC/iPSC-based strategies to treat or model PD, however, is currently hampered by the lack of efficient protocols for the directed differentiation of human pluripotent stem cells into DA neurons with the appropriate characteristics of A9-subtype ventral midbrain neurons, the neuronal cell type lost to PD (for review, see Hwang *et al.*, 2010). A deeper understanding of DA neuron differentiation, patterning, and specialization will surely facilitate the generation of an optimal cell source for cell replacement therapy and disease modeling for PD. During embryo development, midbrain DA neurons originate in the most ventral region of the midbrain and are patterned by local induction through the activity of signaling molecules such as sonic hedgehog (SHH), fibroblast growth factor 8 (FGF8), and wingless (WNT) (for review, see Smidt and Burbach, 2007). As a result of this, a characteristic region-specific makeup of transcription factor expression is established in neural progenitors. Among them, the LIM homeobox transcription factor 1 alpha (Lmx1a) is selectively expressed in the proliferating neural progenitors that give rise to ventral midbrain DA neurons in the mouse, and has been shown to play crucial roles in determining their fate (Andersson *et al.*, 2006). Moreover, overexpression of Lmx1a in mouse embryonic stem cells greatly improved their differentiation toward ventral midbrain DA neurons (Andersson *et al.*, 2006; Cai *et al.*, 2009; Friling *et al.*, 2009), prompting the possibility of using LMX1A modulation to similarly direct the fate of hESC/iPSC-derived neurons. In support of this possibility, *LMX1A* expression was found to be required for the midbrain DA neuron differentiation of hESC (Cai *et al.*, 2009). In spite of these promising pieces of evidence, strategies for increasing DA neuron differentiation of human neural precursors or hESC by *LMX1A* overexpression have been met with limited success. Thus, transfection of *LMX1A*-expressing constructs in human neuroblastoma cell lines did not increase the numbers of tyrosine hydroxylase (TH)-positive neurons (Cai *et al.*, 2009). Similarly, retroviral overexpression of *LMX1A* in immortalized human midbrain progenitors only resulted in very marginal increases in DA neuron differentiation (Roybon *et al.*, 2008).

A possible caveat in previous attempts to overexpress *LMX1A* in human neural stem cells or hESC could be the low levels of transfection/transduction achieved in these notoriously hard-to-transfect cell lines. In this context, the use of lentiviral vectors (LVs) (Naldini *et al.*, 1996), to obtain robust and sustained transgene expression in neural or pluripotent stem cells (Lois *et al.*, 2002; Pfeifer *et al.*, 2002; Ma *et al.*, 2003; Consiglio *et al.*, 2004), acquires particular relevance. Indeed, transduction of hESC-derived neural progenitors with LVs expressing *LMX1A* under the control of a constitutive *phosphoglycerate kinase* (*PGK*) promoter has been recently reported to promote the generation of ventral midbrain DA neurons (Friling *et al.*, 2009).

In this study, we tested whether hESC/iPSC could be stably engineered using LVs so that they would overexpress *LMX1A* in neural progenitors when prompted to differentiate. We show that hESC/iPSC engineered in this way maintain their normal growth characteristics and retain their pluripotent differentiation ability, as judged by *in vitro* differentiation and teratoma formation assays. Notably, the levels of *LMX1A* overexpression achieved in neural progenitors differentiated from engineered hESC/iPSC are sufficient to boost the generation of ventral midbrain DA neurons. Analyses of the phenotypic and physiological properties of these cells, as well as the ability of grafted cells to survive and integrate into the striatum of adult mouse brains, showed that LMX1A-induced DA neurons differentiated from hESC/iPSC are essentially similar to authentic ventral midbrain DA neurons. To the best of our knowledge, this is the first demonstration that LVs can be exploited to stably engineer hESC/iPSC for their directed differentiation toward specific DA neuron phenotypes, thus making it possible to develop new strategies for modeling and treating neurodegenerative diseases.

Materials and Methods

Cell culture

The hESC lines (ES[2] and ES[4]) and the iPSC lines used in these studies have been previously described (Aasen *et al.*, 2008; Raya *et al.*, 2008, 2009). Human pluripotent stem cells were cultured on the top of irradiated (55 Gy) human foreskin fibroblasts (CCD1112SK; ATCC), seeded at a density of 7×10^4 cells/cm^2 on 10-cm cell culture dishes coated with 0.1% gelatin (Chemicon, Millipore, Temecula, CA). The hESC and hiPSC were cultured at 37°C and 5% CO_2 in hESC medium, consisting of KnockOut DMEM (Invitrogen, Paisley, UK) supplemented with 20% KnockOut Serum Replacement (Invitrogen), 0.5% human albumin (Grifols, Barcelona, Spain), 2 m*M* GlutaMAX (Invitrogen), 50 μM 2-mercaptoethanol (Invitrogen), nonessential amino acids (Cambrex, Walkersville, MD), and 10 ng/ml basic fibroblast growth factor (bFGF) (Peprotech, Rock Hill, NJ). Medium was changed every day. Individual hESC and iPSC colonies were passed by mechanical dissociation using a 150-μm-diameter plastic pipette (The Stripper; Midatlantic Diagnostics, Mount Laurel, NJ) and replated every 5–7 days. Karyotyping was

performed by incubating colonies for 30 min in 2 μl/ml Colcemid (Invitrogen) by the G-banding method. Fifteen metaphases were analyzed for each line.

Plasmid construction, lentiviral production, and hESC and iPSC transduction

LMX1A or green fluorescent protein (GFP) expression was driven by the *NESTIN* enhancer (NesE) (1,852 bp) and the basic herpes virus thymidine kinase (HSV tk) promoter element (925 bp). This enhancer contains a sufficient *cis*-element that recapitulates endogenous *NESTIN* expression in the CNS (Lothian and Lendahl, 1997). The cassette containing the NesE, HSV tk promoter, and Lmx1a cDNA was cloned in the CSC.cPPT.hCMV.GFP.Wpre LV backbone previously described (Lie *et al.*, 2005). High-titer vesicular stomatitis virus (VSV)–pseudotyped LV stocks were produced in 293T cells by calcium phosphate–mediated transient transfection of the transfer vector pRRL-SIN-PPT-*NesE*-Lmx1a-ires-GFP-WPRE, the late generation packaging construct pMDL, and the VSV envelope–expressing construct pMD2.G, and purified by ultracentrifugation as previously described (Consiglio *et al.*, 2004). Expression titers, determined using HeLa cells by FACS analysis, were 5×10^8 to 1×10^9 transducing units (TU)/ml with an average HIV-1 p24 concentration of 100 μg/ml. The same day of transduction, 2×10^5 hESC (passage 15) were infected in suspension at multiplicity of infection (MOI) of 10 with LV.NES.LMX1A.GFP, LV.NES.GFP, or LV.PGK.GFP in the presence of 6 μg/ml Polybrene (Sigma, Sigma-Aldrich Co, St. Louis, MO). The day after transduction, the medium was changed and transduction efficiency was estimated by FACS analysis for GFP expression.

DA differentiation of hESC

For neural induction, embryoid bodies (EBs) were generated from large colony fragments obtained by mechanical splitting with a finely drawn Pasteur pipette and cultured in nonadherent dishes for 3–4 days in the presence of hES medium. At Stage 2, EBs were cultured 10 days in suspension in N2B27 medium consisting of DMEM/F12 medium (Invitrogen), Neurobasal medium (Invitrogen), 0.5× B-27 supplement (Invitrogen), 0.5× N2 supplement (Invitrogen), 2 m*M* GlutaMAX (Invitrogen), and penicillin–streptomycin (Invitrogen). In this stage, N2B27 medium was supplemented with 10 ng/ml bFGF, 100 ng/ml FGF8 (Peprotech), and 100 ng/ml SHH (Invitrogen). Finally, at Stage 3 for DA neuron maturation, the neural precursors cells (NPCs) were cocultured with PA6 for 3 weeks in N2B27 medium supplemented with FGF8 and SHH.

In vitro *differentiation toward the embryonic germ layers*

Differentiation toward endoderm, mesoderm, and neuroectoderm was carried out essentially as described (Raya *et al.*, 2010).

Teratoma formation in nude mice

Severe combined immunodeficient (SCID) beige mice (Charles River Laboratories) were used to test the teratoma induction capacity of hES-LMX1A cells essentially as described (Raya *et al.*, 2008). All animal experiments were conducted following experimental protocols previously approved by the Institutional Ethics Committee on Experimental Animals, in full compliance with Spanish and European laws and regulations. In brief, $\sim1–3\times10^6$ hES-LMX1A cells were injected subcutaneously into the testis of SCID mice anesthetized with isoflurane. Five to 8 weeks after injection, teratomas were dissected, fixed overnight in 10% buffered formalin phosphate, and embedded in paraffin.

RT-PCR analysis

Total mRNA was isolated by guanidinium thiocynate–phenol–chloroform extraction (TRIzol; Invitrogen) and treated with DNase I. One microgram was used to synthesize cDNA by using the SuperScript III Reverse Transcriptase Synthesis Kit (Invitrogen). Quantitative PCR (qPCR) analysis was done in triplicate on 50 ng by using Platinum SYBER Green qPCR SuperMix (Invitrogen) in an ABI Prism 7000 thermocycler (Applied Biosystems). All results were normalized to the average expression of hypoxanthine phosphoribosyltransferase (*HPRT*) and *B-2-MICROGLOBULIN.* Results were obtained from three or four technical replicates of three or four independent biological samples at each data point. Transcript-specific primers used were as follows: B2M, 5′-GCCGTGTGAACCATGTGACT-3′ and 5′-GCTTACATGT CTCGATCCCACTT-3′; HPRT, 5′-TATGGACAGGACTGA ACG TCTTG-3′ and 5′-GCACACAGAGGGCTACAATGTG-3′; LMX1A, 5′-AGGAAGGCAA GGACCATAAGC-3′ and 5′-ATGCTCGCCTCTGTTGAGTTG-3′; PAX6, 5′-GCTTCAC CATGGCAAATAACC-3′ and 5′-GGCAGCATGCAGGAG TATGA-3′; SOX1, 5′-TACGT TTATTTCAGCAGCCTTAGG-3′ and 5′-TCCAGGACAAGGAAGGGTGTT-3′; NURR1, 5′-CGCCTGTAACTCGGCTGAAG-3′ and 5′-CTTGAGGCGAG GACCCATAC-3′; ALDH1A1, 5′-TGACAAGATCCAGGGC CGTACAAT-3′ and 5′-TGAGAGGAGTTTGC TCTGCTG GTT-3′; EN1, 5′-CAGACCCATAATCCTGCATTTCTC-3′ and 5′-TTTGGGA TGTAGGCAAATGGA-3′; OCT4, 5′-GGA GGAAGCTGACAACAATGAAA-3′ and 5′-GGCCTGCACG AGGGTTT-3′; NANOG, 5′-ACAACTGGCCGAAGAATA GCA-3′ and 5′-GGTTCCCAGTCGGGTTCAC-3′; TH, 5′-CCG AGCTGTGAAGGTGTTTGA-3′ and 5′-CGGGCCGGGTC TCTAGAT-3′; IRES, 5′-TGTGAGGGCCCGGAAAC-3′ and 5′-GGGAAAGACCCCTAGGAATGC-3′; UTR, 5′-CCTTGG CTCTTCCTTCCAACT-3′ and 5′-ATGGCTGCTGGGTCTTC TGT-3′.

DNA extraction, Southern, and integration analysis

DNA isolation was performed with the DNeasy Blood & Tissue kit (Invitrogen) according to the manufacturer's instructions. For Southern analysis, the genomic DNA was digested overnight with 40 U of *Pst*I restriction enzyme (New England Biolabs, Ipswich, MA), electrophoresed on a 1% agarose gel, transferred to a neutral nylon membrane (Hybond-N; Amersham, GE Healthcare Limited, Buckingham-Shire) by capillary transfer, and hybridized with a GFP digoxigenin (DIG)–2′-deoxyuridine 5′-triphosphate–labeled probe generated by PCR using the PCR DIG Probe Synthesis Kit (Roche Diagnostics, GmbH, Mannheim, Germany). The probe was detected by an alkaline phosphatase–conjugated DIG-Antibody (Roche Diagnostics) using CDP-Star (Sigma-Aldrich) as a substrate for chemiluminescence. The GFP

probe was generated using an eGFP template with the primers GFP-F 5′-CGCACCATCTT CTTCAAGGAC-3′ and GFP-R 5′-CATGCCGAGAGTGATC CCG-3′.

Quantification of transgene copy number per cell was analyzed by qPCR using Platinum SYBER Green qPCR SuperMix (Invitrogen) in an ABI Prism 7000 thermocycler (Applied Biosystems, Life Technologies, Paisley, UK). To determine the number of integrations, primers specific for the transgene sequence were generated: IRES-F, 5′-TGTGAG GGCCCGGAAAC-3′ and IRES-R 5′-GGGAAAGACCCC TAGGAATGC-3′. To quantify the number of cells, *B-ACTIN* primers were used: B-ACTIN-F 5′-ATTGGCAATGAGCG GTTCC-3′ and B-ACTIN-R 5′-ACA GTCTCCACTCACCC AG GA-3′. To measure the average proviral DNA per transduced cell, two standard curves were made: one employing a known amount of the LV (LV.NES.LMX1A.GFP) using the IRES primers, and a second curve employing a known number of cells and the *B-ACTIN* primers. Next, the average proviral number per cell was estimated by interpolation of the IRES-to-*B-ACTIN* ratio from each DNA sample in the two standard curves.

Immunochemistry and cell counts

hESC and iPSC were grown on plastic cover-slide chambers for immunostaining. Cells were fixed with 4% paraformaldehyde and then permeabilized with 0.5% Triton X-100 in Tris-buffered saline. Cells were then blocked in 0.5% Triton X-100 with 3% donkey serum for 2 hr before incubation with primary antibody overnight at 4°C. The following antibodies were used: mouse anti-Tra-1-60 (Chemicon; 1:100), mouse anti-Tra-1-81 (Chemicon; 1:100), rabbit anti-Sox2 (Chemicon; 1:500), rabbit anti-GAD (Chemicon; 1:1,000), mouse anti-HNA (Chemicon; 1:200), rabbit anti-calbindin (Chemicon; 1:1,000), rabbit anti-Nestin (Chemicon;1:200), rat anti-DAT (Millipore; 1:400, Hudson, WI), mouse anti-SSEA-4 (MC-813-70, 1:2), and mouse anti-SSEA-3 (MC-631, 1:2) (from the Developmental Studies Hybridoma Bank at the University of Iowa), rabbit anti-TH (Sigma; 1:1,000), rabbit anti-Girk2 (Sigma; 1:40), mouse anti-ACTA1 (Sigma; 1:400), mouse anti-SMA (Sigma; 1:400), rabbit anti-α-fetoprotein (1:400), rabbit anti-GFAP (Dako; 1:1,000, Dako, Denmark), mouse anti-Tuj1, (Covance; 1:500, Emeryville, California), mouse anti-Oct-3/4 (Santa Cruz; 1:100), rabbit anti-Gata4 (Santa Cruz; 1:50), goat anti-Nanog (Everest Biotech; 1:100, Oxford-Shire, UK), goat anti-FoxA2 (R&D Biosystems; 1:100), chicken anti-GFP (AveLabs; 1:200), rabbit anti-5-HT (Immunostar; 1:2,000), mouse anti-synaptophysin (Millipore; 1:500, Hudson, WI), rabbit anti-DBH (Chemicon; 1:200), and rabbit anti-Lmx1a (kindly provided by Dr. M.S. German, University of California, San Francisco Diabetes Center). Secondary antibodies used were all the Alexa Fluor Series from Invitrogen (all 1:500). Images were taken using a Leica SP5 confocal microscope. For quantification of stained cells, 300 cells per differentiated aggregate were randomly counted (average six to eight differentiated aggregates per experiment). Data points represent the average of at least three independent experiments.

Transplantation in immunodeficient mice

Twenty 6-week-old SCID beige mice were anesthetized and stereotaxically injected with 2×10^5 cells at Stage 3 in 2 μl using a Hamilton syringe in the striatum. The cells were injected at 1 μl/min rate. Mice were sacrificed at 1 month ($n=11$) and 5 months ($n=8$) after transplantation. Upon sacrifice, animals were perfused transcardially with paraformaldehyde (4%), and the brains sectioned at 20 μm on a freezing microtome and stained with antibodies as previously described. Brain sections were analyzed for the presence of immunoreactive cells along the entire length of the graft. All animal experiments were conducted following experimental protocols previously approved by the Institutional Ethics Committee on Experimental Animals, in full compliance with Spanish and European laws and regulations.

DA enzyme-linked immunosorbent assay (ELISA)

Levels of DA were quantified using an ELISA kit obtained from Rocky Mountain Diagnostics (Colorado Springs, CO; http://www.rmdiagnostics.com) according to the manufacturer's instructions. In brief, after being rinsed in a low-KCl (4.7 m*M*) solution, the cells were incubated in 1 ml of a high-KCl (60 m*M*) solution for 15 min at 37°C. After stimulation with high potassium, DA was measured by ELISA analysis, as previously described (Trzaska *et al.*, 2007).

Electrophysiology recordings

Electrophysiology studies were performed using E^2 Technology (Aleria Biodevices, Barcelona, Spain). In brief, the cells are cultured in a plate composed of pairs of wells connected through a 1-mm-long microchannel, cells are seeded in the wells, and axons sprout all along the microchannel. For recording, one electrode is located in each well. NPCs were seeded in the wells on the top of PA6; 3 weeks later, recordings in loose-patch mode were obtained (Morales *et al.*, 2008).

Statistical analysis

Data were statistically analyzed by Student's *t* test using Microsoft Excel software as indicated.

Results

In vitro *differentiation of DA neurons from hESC/iPSC*

In a first series of experiments, we used the ES[4] hESC line previously derived in our laboratory (Raya *et al.* 2008), maintained by mechanical passaging on top of feeder layers of irradiated human foreskin fibroblasts. To promote DA neuron differentiation, we implemented a three-stage protocol involving (1) hESC aggregation (via EB formation), (2) neural induction, and (3) DA neuron maturation using a PA6 feeder-based system (Kawasaki *et al.*, 2002) (Fig. 1a). Specifically, neural induction was carried out by incubating EBs in suspension for 10 days in a defined medium supplemented with FGF2, SHH, and FGF8 (Ying *et al.*, 2003; Roy *et al.*, 2006) (Fig. 1b). After that, in Stage 2, NPCs positive for early neural markers, such as NESTIN and SOX2, started to become apparent in the dish (Fig. 1c and d). To achieve DA neuron maturation, NPCs were then treated in Stage 3 with FGF8/SHH and plated on top of PA6 cells. At this stage and under these conditions, almost 50% of the cells expressed the neuronal marker TUJ1, of which ~50% were of DA lineage as judged by TH expression (Fig. 1e). In our hands, differentiation of hESC in monolayer (*e.g.*, without EB formation) or in

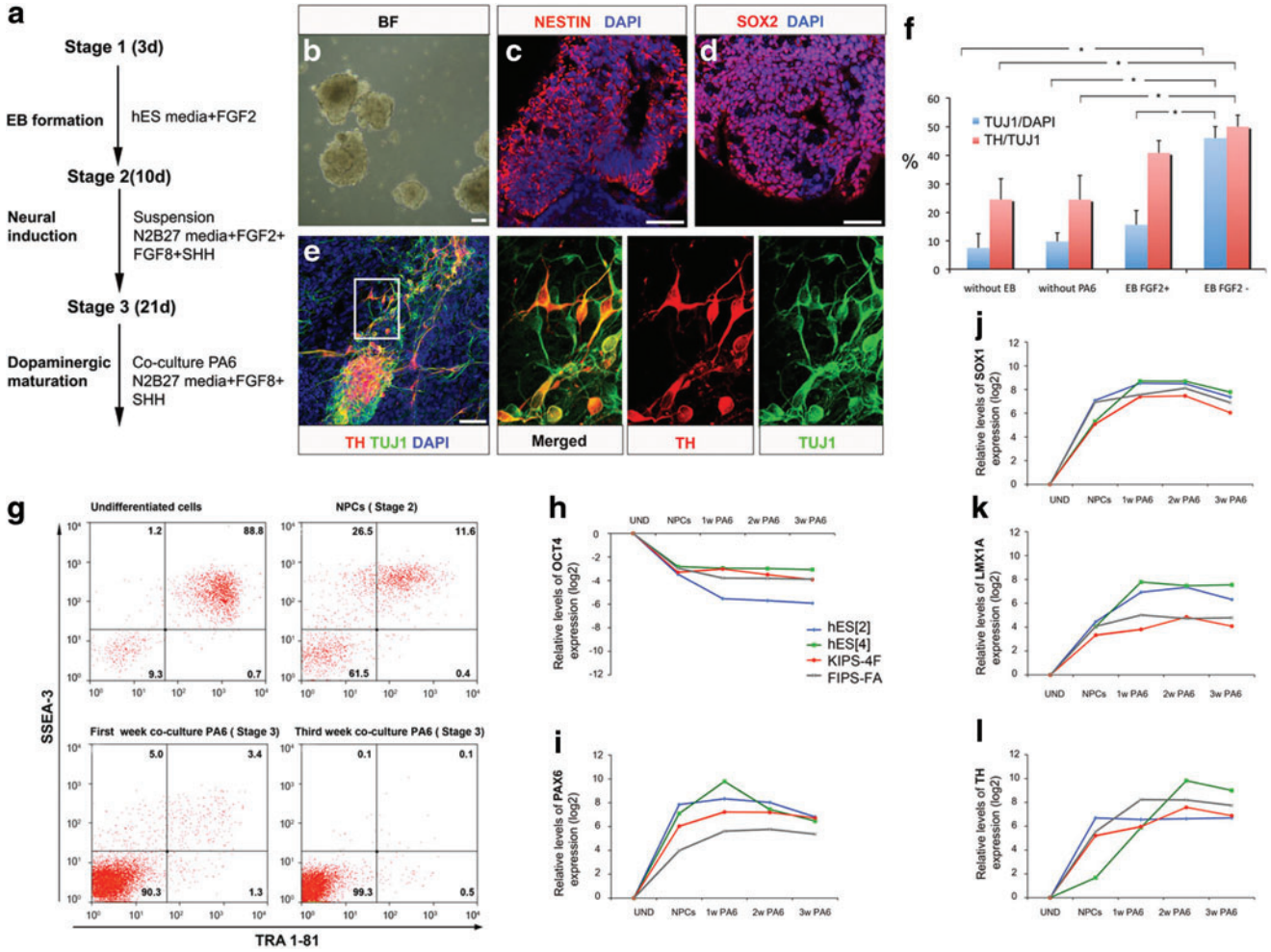

FIG. 1. Differentiation protocol implemented for the generation of DA neurons and validation of specific expression of LMX1A in neural precursor cells. **(a)** Schematic representation of the different stages for the *in vitro* differentiation of pluripotent stem cells toward DA neurons. At Stage 1, EBs are formed by aggregation. At Stage 2, NPCs are obtained culturing the EBs in suspension with N2B27 medium supplemented with FGF2, FGF8, and SHH. At Stage 3, NPCs are cocultured with PA6 for 3 weeks and DA neurons are generated. **(b)** NPCs formed at Stage 2 express the neural precursor markers NESTIN **(c)** and SOX2 **(d)**. **(e)** At Stage 3, some of the TUJ1-positive cells generated coexpress TH. **(f)** Omitting the EB generation step or the coculture with PA6 cells results in <10% of the cells differentiating to neurons, of which ~24% are TH-positive. Better results are obtained with the addition of FGF2 during the coculture with PA6; the number of neurons generated is 14% and 40% of the neurons stained for TH. With the three-stage protocol implemented in (a), the yield of neurons generated increases to 48% and the TH-positive neurons to 50%. **(g)** Flow cytometry analysis shows that, in the undifferentiated state, 90% of the cells are positive for TRA-1-81 or SSEA-3. This value is reduced to 38% in NPCs and to 10% at the first week in coculture with PA6. At 3 weeks in coculture with PA6, 99% of the cells are double negative, thus indicating that mainly all of the cells have entered into the differentiation process. **(h)** A decrease or inactivation of the expression of the pluripotency marker *OCT4* is found as the differentiation occurs. **(i, j)** The neural precursor markers *PAX6* and *SOX1* show activation in NPCs, and the expression starts to decay at 3 weeks in coculture with PA6. **(k)** The DA progenitor marker *LMX1A* starts to be expressed in NPCs, but reaches the maximum level of expression during coculture with PA6. **(l)** *TH* levels of expression are first detected in NPCs, and its expression is maintained or grows until the end of the protocol. $*p < 0.05$. Scale bar = 50 μm. In all experiments, $n = 3$. Color images available online at www.liebertonline.com/hum

the absence of PA6 coculture resulted in poor DA neuron yield (<10% of the differentiated cells were neurons, of which <25% were DA neurons; Fig. 1f). Similarly, supplementation with FGF2 during the entire differentiation protocol resulted in fewer neurons and DA neurons compared with conditions where FGF2 was withdrawn during Stage 3 (Fig. 1f).

As expected, the expression of SSEA-3 and TRA-1-81, markers of undifferentiated hESC, dramatically declined during the differentiation process, so that only 0.1% of the cells expressed both markers at the end of the protocol, as judged by flow cytometry (Fig. 1g). We confirmed these results by real-time quantitative RT-PCR analyses of *OCT4* expression, which also showed a marked decrease as differentiation proceeded (Fig. 1h). To test whether our differentiation protocol could be applied to other lines of human pluripotent stem cells with comparable results, we subjected an additional hESC line {ES[2] (Raya *et al.*, 2008)} and two

independent lines of iPSC [KiPS4F#1 and cFA404FiPS4F#1 (Aasen *et al.*, 2008; Raya *et al.*, 2009, respectively)] to the same protocol and harvested samples at different time points for analyses of gene expression. The behavior of all four hESC/iPSC lines was similar in terms of the decrease in *OCT4* expression and the up-regulation of neural and neuronal markers (Fig. 1h). Specifically, markers of neural precursors such as *PAX6* and *SOX1* were found up-regulated in all cell lines tested, peaking at the end of Stage 2 or the first week of Stage 3, whereas markers of DA neuron phenotype such as *TH* peaked at later time points. The expression of *LMX1A*, encoding a key transcription factor for midbrain identity (Andersson *et al.*, 2006), showed an intermediate profile, with maximum levels reached between weeks 2 and 3 of Stage 3 (Fig. 1i–l). These results show that we have optimized a protocol for DA neuron differentiation from human pluripotent stem cells that is applicable to both hESC and iPSC, and that achieves DA neuron differentiation efficiencies in the range of previously published protocols (for review, see Hwang *et al.*, 2010). However, and also in agreement with previous reports (for review, see Hwang *et al.*, 2010), DA neurons generated with our protocol were not the majority of the specific subtype lost in PD (*i.e.*, A9-subtype ventral midbrain DA neurons), as judged by the expression of G protein–activated inward rectifier potassium channel 2 (GIRK2; encoded by *potassium channel, inwardly rectifying, subfamily j, member 6; KCNJ6*) (Inanobe *et al.*, 1999; Mendez *et al.*, 2005) (see below).

Achieving neural-specific overexpression of LMX1A

Therefore, we next asked whether delivering the ventral midbrain DA lineage-associated transcription LMX1A to human pluripotent stem cells could provide appropriate regionalization cues during their differentiation. For this purpose, we generated an LV (LV.NES.LMX1A.GFP; Fig. 2a) in which *LMX1A* expression is driven by a neural *NESTIN* enhancer, active in neural progenitor cells (Lothian and Lendahl, 1997) and a minimal *TK* promoter. The vector also expressed GFP downstream of an IRES element, to allow monitoring of the transgenic expression of *LMX1A* during the differentiation process. After transduction of hESC with this LV at an MOI of 50, GFP expression was not observed in undifferentiated hESC, whereas it could be clearly detected by epifluorescence microscopy or flow cytometry during the early steps of neural differentiation (Fig. 2b and c). In contrast, >90% of hESC transduced in parallel with LVs expressing GFP from a constitutive PGK promoter (LV.PGK.GFP) displayed strong GFP expression in both the undifferentiated state and during neural differentiation (Fig. 2b and c). The specificity of the LV.NES.LMX1A.GFP construct in hESC undergoing neural differentiation was further confirmed by testing coimmunolocalization of GFP and NESTIN (Fig. 2d).

To investigate the effect of *LMX1A* overexpression during the differentiation of human pluripotent stem cells, we subjected hESC tranduced with LV.NES.LMX1A.GFP to our three-stage DA neuron differentiation protocol, and compared the overall yield of neurons and DA neurons with those of hESC transduced with a control (LV.NES.GFP) virus. Whereas no overt differences were found in the total number of neurons in each condition at the end of Stage 3, hESC overexpressing *LMX1A* generated a significantly higher proportion of DA neurons (Fig. 2e). However, the increased DA neuron differentiation of LV.NES.LMX1A.GFP-transduced hESC was progressively lost as cells were passaged (Fig. 2e), concomitant with a decrease in the levels of transgenic *LMX1A* overexpression (Fig. 2f), suggesting silencing of the LV transgenes and/or selection of untransduced hESC upon passaging.

Generation of hESC clones overexpressing LMX1A

To circumvent the loss of *LMX1A* expression in bulk-transduced hESC, we set out to generate clonal lines of LV.NES.LMX1A.GFP-transduced hESC (hES-LMX1A cells). As controls, stable cell lines transduced with LV.NES.GFP were generated (mock-hESC). In order to obtain hESC colonies derived from single cells, 5 days after infection (MOI 10) cells were trypsinized to single cells and serial dilutions plated on human feeder fibroblasts in six-well plates. Between 3 and 6 weeks after plating, colonies of tightly packed cells with a high nucleus-to-cytoplasm ratio and hESC-like morphology appeared in those cultures. We picked and expanded nine independent colonies from wells in which only two to four colonies had grown. The number of lentiviral integration(s) in each clonal line were first screened by qPCR on genomic DNA using primers specific to the IRES sequence and normalized for β-actin (see Materials and Methods for details). From the nine clones analyzed, five of them (clones A, C, G, H, and K) showed no lentiviral integrations, three of them (clones B, L, and I) contained a single lentiviral integration, and one (clone D) showed two integrations. The accuracy of this PCR-based screen was confirmed in selected clones by Southern blot hybridization (Fig. 3a). We selected clones D and L of transgenic hES-LMX1A cells for a thorough characterization and first tested whether the LV transduction could support undifferentiated hESC culture for extended periods of time. After 32 passages, or 8 months in continuous culture, transgenic hES-LMX1A cells maintained a normal 46-XY karyotype (Fig. 3b and data not shown) and remained undifferentiated and pluripotent, as judged by the expression of pluripotency-associated markers OCT4, NANOG, and SOX2, and surface markers SSEA-3, SSEA-4, TRA-1-81 (Fig. 3c–e and data not shown), and the ability to differentiate *in vitro* into derivatives of the three main embryonic germ layers (Fig. 3f–h and data not shown). In addition, injection of clone D hESC into immunocompromised mice resulted in complex teratomas containing derivatives from all three germ layers, further confirming that transgenic hES-LMX1A cells were pluripotent (Fig. 3i–k). Overall, these results show that genetic manipulation of hESC with LVs expressing *LMX1A* under the control of a neural *NESTIN* enhancer does not cause any conspicuous deleterious effect in their self-renewing or pluripotent differentiation abilities.

Effect of neural-specific overexpression of LMX1A on DA neuron differentiation

Transgenic clones of hES-LMX1A cells showed a robust overexpression of *LMX1A* under DA neuron differentiation conditions, reaching levels of up to 10-fold higher than those of mock-hESC (Fig. 4a). During the course of DA neuron differentiation, both hES-LMX1A and mock-hESC showed

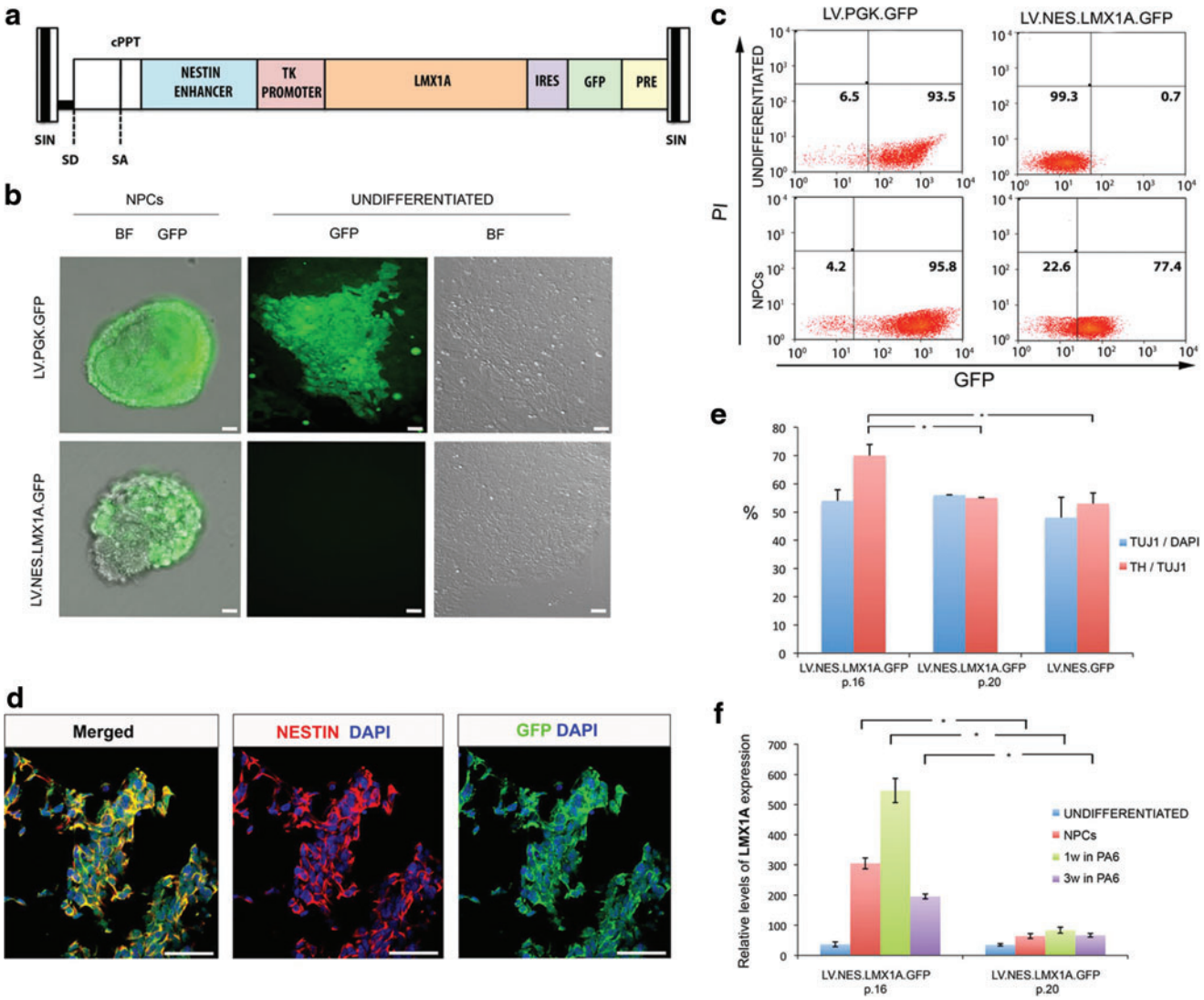

FIG. 2. Ectopic LMX1A is specifically expressed in neural precursor cells. **(a)** Schematic representation of the proviral form of LV.NES.LMX1A.GFP, in which the expression of LMX1A and the reporter GFP is driven by the activation of the NESTIN enhancer. **(b)** Bright-field and fluorescent images showing no expression of GFP in the undifferentiated cells infected with LV.NES.LMX1A.GFP and expression of GFP in NPCs from cells infected with LV.NES.LMX1A.GFP. GFP is present in undifferentiated and NPCs from cells infected with LV.PGK.GFP. **(c)** Flow cytometry analysis for GFP. More than 93% of the cells infected with LV.PGK.GFP present GFP expression in an undifferentiated state and NPCs. Of the cells infected with LV.NES.LMX1A.GFP, almost none are positive for GFP in the undifferentiated state, but ~77% of the NPCs are GFP-positive. **(d)** NPCs infected with LV.NES.LMX1A.GFP coexpress NESTIN and GFP. **(e)** Quantification of the neuronal and dopaminergic yield at Stage 3. Cells infected with LV.NES.LMX1A.GFP show in four passages a decrease in the amount of TH-positive neurons from 70% to 55%, the latter value having been obtained using LV.NES.GFP. The number of neurons obtained in all the cases is ~55%. **(f)** *LMX1A* expression is markedly decreased at passage 20 compared with that at passage 16. *$p < 0.05$. Scale bar = 50 μm. In all experiments, $n = 3$. Color images available online at www.liebertonline.com/hum

a progressive decline in the expression of pluripotency-associated genes such as *NANOG*, until levels were barely detectable (Fig. 4b). However, the increase in the expression of genes associated with DA neuron differentiation, such as *nuclear receptor subfamily 4, group a, member 2* [*NR4A2*, encoding nuclear receptor-related 1 (NURR1)], *engrailed 1* (*EN1*), *aldehyde dehydrogenase 1* (*ALDH1A1*), and *TH*, was significantly more pronounced in hES-LMX1A cells when compared with mock-hESC (Fig. 4c–f), suggesting that more cells were being specified to a DA neuron lineage. We directly addressed this possibility by analyzing the expression of relevant markers (Isacson *et al.*, 2003) at various time points of the differentiation protocol by immunofluorescence (Fig. 4g–p). As expected, more LMX1A-positive cells were found in differentiating hES-LMX1A cells in comparison with mock-hESC at Stage 2 (Fig. 4g and h). Moreover, at the end of Stage 3, hES-LMX1A cells generated >25% more DA neurons than mock-hESC (Fig. 4i and j), as evaluated by quantifying the number of TH/TUJ1 double-positive cells (Fig. 4q). Importantly, the majority of DA neurons differentiated from hES-LMX1A cells, but not from mock-hESC, presented the typical bipolar morphology of mDA neurons,

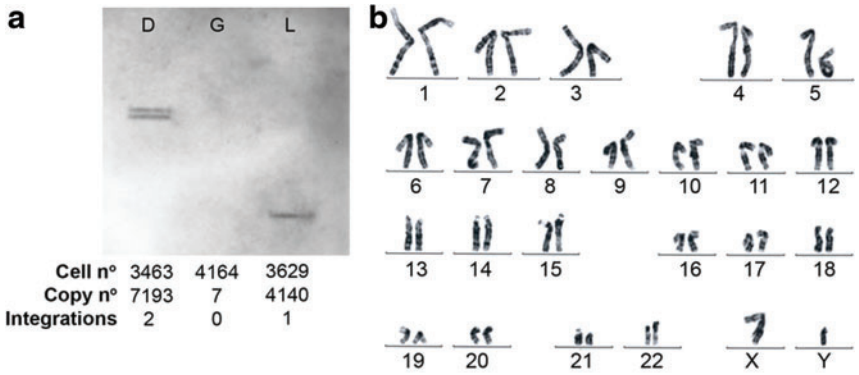

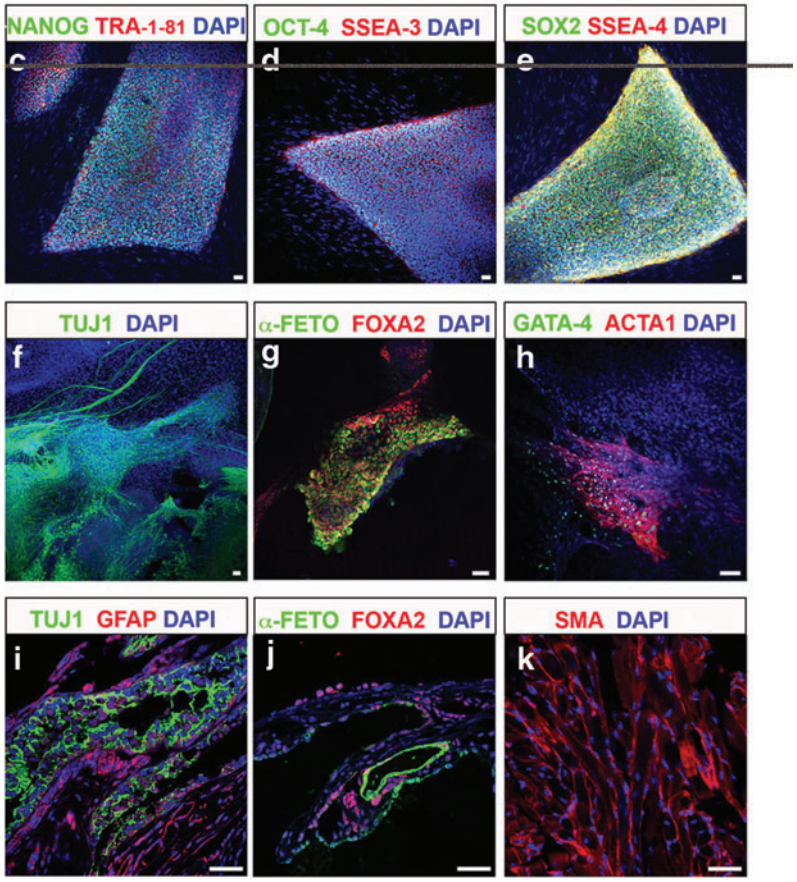

FIG. 3. Generation of hESC clones overexpressing *LMX1A*. **(a)** Southern blot analysis of clones D, G, and L using a probe against LMX1A informing about the lentiviral integration copy number. Integration results using qPCR confirm the results obtained in the Southern blot. **(b)** The transduced clone D showed normal karyotype. **(c–e)** After the infection, clone D retains the pluripotency capacity as judged by the expression of pluripotency markers NANOG, TRA-1-81, OCT-4, SSEA-3, SOX2, and SSEA-4. The ability to give rise to the three germ layers *in vitro* **(f–h)** and *in vivo* **(i–k)** is also shown. Scale bar = 50 μm. Color images available online at www.liebertonline.com/hum

FIG. 4. LMX1A enhances generation of midbrain DA neurons in hESC. **(a)** qPCR analysis for relative levels of *LMX1A* expression showing overexpression of *LMX1A* in hES-LMX1A (clone D) compared with mock-hESC. Relative levels of expression of the pluripotency marker *NANOG* **(b)** are similar in both lines. Higher levels of *NURR1* **(c)**, *EN1* **(d)**, *ALDH1A1* **(e)**, and *TH* **(f)** are observed in hES-LMX1A compared with mock-hESC. **(g–w)** hESC are differentiated and analyzed at different stages of the DA protocol. **(g, h)** Staining for LMX1A at Stage 2 is more prominent in hES-LMX1A than in mock-hESC. Staining at the end of the protocol for TH and TUJ1 **(i, j)**, TH and GIRK2 **(k, l)**, and TH and DAT **(m, n)**, show a higher number of TH-, GIRK2-, and DAT-positive neurons in hES-LMX1A as compared with mock-hES. Only hES-LMX1A in Stage 3 present TH-positive neurons with staining of FOXA2 in the nucleus, a feature typical of mDA neurons but not mock-hES **(o, p)**. **(q)** Quantification of TUJ1, TH, and GIRK2 expression at the end of the protocol. The expression of TUJ1 is ~55% in both infected lines. Approximately 55% of mock-hESC TUJ1-positive cells expressed TH, and this amount increased to 80% in hES-LMX1A. The expression of GIRK2, a midbrain DA neuron marker, is restricted to 20% of the cells from mock-hESC and present in the majority of TH-positive neurons from hES-LMX1A. **(r–w)** Analyses for other neuronal subtypes within the culture at the end of the protocol. **(r)** Some TH-positive neurons are positive for calbindin in mock-hES, indicating that they are A10 neurons. In contrast, in hES-LMX1A, there is no costaining for TH and calbindin **(s)**. **(t, u)** Absence of DBH-positive neurons within the culture. **(v, w)** Absence of 5-HT-positive neurons within the culture. **(x)** DA release analysis exhibiting release of DA after treatment with high KCl only in the differentiated DA neurons and not in undifferentiated cells. **(y)** Electrophysiological analysis showed presence of action potentials in cells at Stage 3. In DA neurons from hES-LMX1A, a change in the frequency of action potentials could be observed when DA was added to the medium; no change was detected in the neurons from mock-hESC. In all experiments, $n = 3$. *$p < 0.05$. Scale bar = 50 μm. Color images available online at www.liebertonline.com/hum

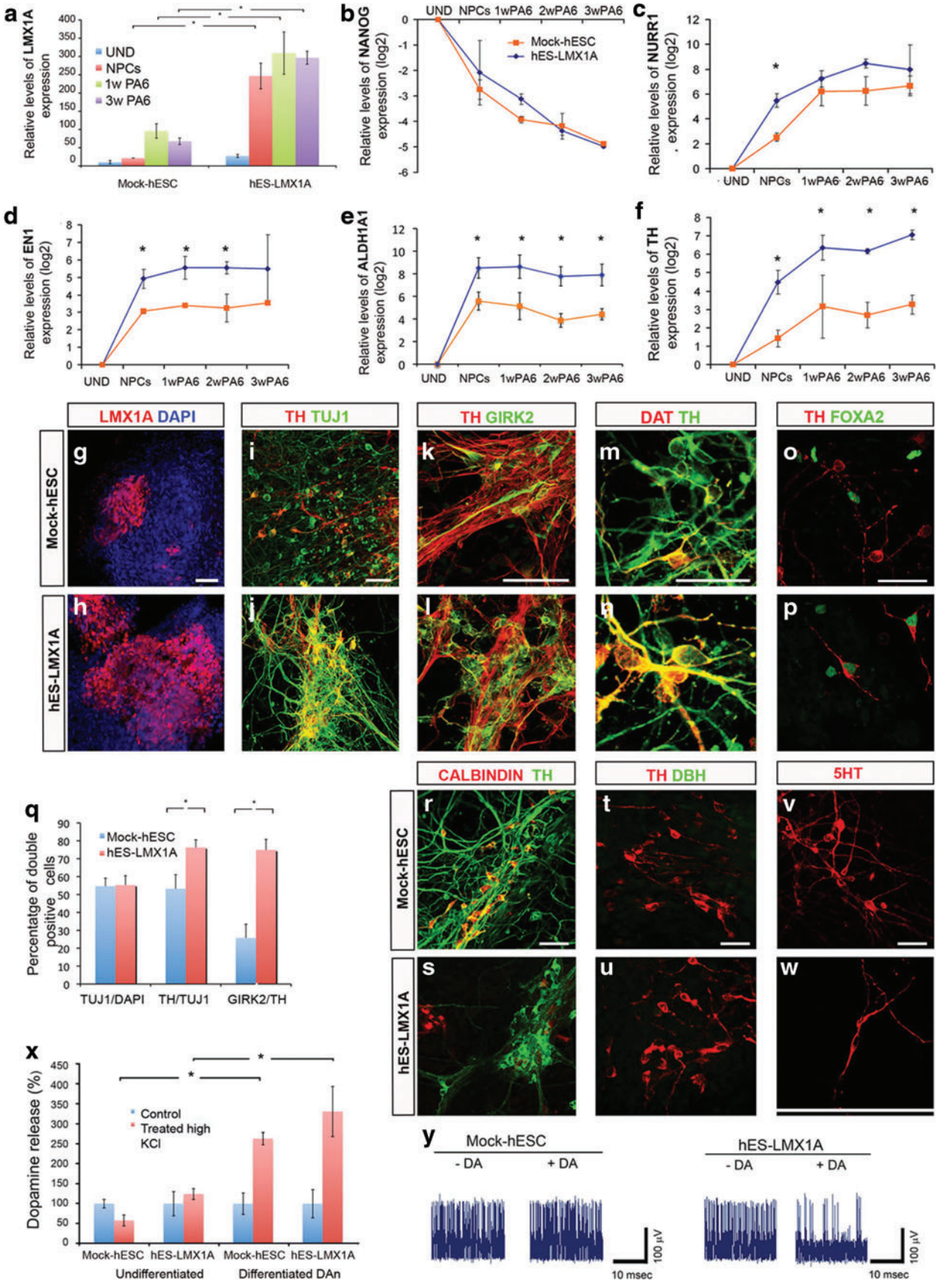
a
Relative levels of LMX1A expression
UND
NPCs
1w PA6
3w PA6
Mock-hESC
hES-LMX1A
b
Relative levels of NANOG expression (log2)
UND NPCs 1wPA6 2wPA6 3wPA6
Mock-hESC
hES-LMX1A
c
Relative levels of NURR1 expression (log2)
UND NPCs 1wPA6 2wPA6 3wPA6
d
Relative levels of EN1 expression (log2)
UND NPCs 1wPA6 2wPA6 3wPA6
e
Relative levels of ALDH1A1 expression (log2)
UND NPCs 1wPA6 2wPA6 3wPA6
f
Relative levels of TH expression (log2)
UND NPCs 1wPA6 2wPA6 3wPA6
LMX1A DAPI
TH TUJ1
TH GIRK2
DAT TH
TH FOXA2
Mock-hESC
hES-LMX1A
g
h
i
j
k
l
m
n
o
p
CALBINDIN TH
TH DBH
5HT
r
s
t
u
v
w
q
Percentage of double positive cells
Mock-hESC
hES-LMX1A
TUJ1/DAPI
TH/TUJ1
GIRK2/TH
x
Dopamine release (%)
Control
Treated high KCl
Mock-hESC hES-LMX1A Mock-hESC hES-LMX1A
Undifferentiated
Differentiated DAn
y
Mock-hESC
- DA
+ DA
hES-LMX1A
- DA
+ DA
100 µV
10 msec
100 µV
10 msec

stained positive for FOXA2, coexpressed the A9-subtype marker GIRK2, and were mature, as judged by coexpression of DA transporter (DAT) (Fig. 4k–p). In contrast, DA neurons differentiated from hES-LMX1A cells did not express the A10-subtype marker calbindin, although some calbindin-expressing neurons were observed, whereas this marker was frequently coexpressed in mock-hESC-derived DA neurons (Fig. 4r and s). DA neurons differentiated from either hES-LMX1A cells or mock-hESC did not express the marker of adrenergic neurons dopamine-β-hydroxylase (DBH, Fig. 4t and u), or serotonin (5-HT), marker of serotonergic neurons (Fig. 4v and w).

Functional characterization of DA neurons differentiated from hES-LMX1A cells

We next tested whether DA neurons allowed to differentiate fully *in vitro* (end of Stage 3) displayed the functional characteristics expected from *bona fide* DA neurons. For this purpose, we analyzed their ability to release DA in response to appropriate stimuli. Cells differentiated from either hES-LMX1A or mock-hESC (but not undifferentiated cells) showed robust DA release induced by a depolarizing solution of KCl (60 m*M*; see Fig. 4x). Next, we analyzed the electrophysiological properties of DA neurons through extracellular recordings using the E^2 Technology, in which 10–50 axons grow within a microchannel and allow simultaneous recording of multiple neurons (Morales *et al.*, 2008). These studies showed that cells differentiated from either hES-LMX1A or mock-hESC, but not undifferentiated cells, fired spontaneous action potentials, providing evidence that these cells are, indeed, functional neurons. Moreover, cells differentiated from hES-LMX1A, but not from mock-hESC, responded to the application of DA with a marked reduction in spontaneous firing activity (Fig. 4y), a behavior characteristic of midbrain DA neurons (Friling *et al.*, 2009). Taken together, our results so far show that clones of hESC engineered to overexpress *LMX1A* in neural precursors, when subject to our optimized protocol for DA neuron differentiation, efficiently generate DA neurons that are molecularly and functionally of the ventral midbrain A9 subtype.

To investigate the functional properties of DA neurons differentiated from hES-LMX1A and mock-hESC, we first tested their ability to engraft and survive within the context of the adult brain. For this purpose, we transplanted 2×10^5 differentiating hESC at mid-Stage 3 (after 2 weeks of coculture with PA6 cells) directly into the striatum of unlesioned mice. One month after transplantation, grafted cells identified by GFP expression (Fig. 5a), immunofluorescence against TUJ1/TH (Fig. 5b), and antibodies against human nuclear antigen (HNA) (Fig. 5c) were found at the expected position in 10 of 11 mice. To analyze longer grafting times, we retained four mice injected with mock-hESC and four mice injected with hES-LMX1A cells for an additional 4 months. In all eight animals, we found viable grafts containing human TH-positive cells (Fig. 5d–f), although their numbers were much higher in those injected with hES-LMX1A cells (compare Fig. 5e and f). Moreover, confocal immunofluorescence microscopy showed that the vast majority of TH-positive cells found in the engrafted hES-LMX1A cells 5 months after transplantation were mature A9-subtype DA neurons, as shown by coexpression of GIRK2 and DAT (Fig. 5g). Consistent with this, we did not detect GABAergic or serotonergic neurons in the grafted area (Fig. 5h and i).

Effect of LMX1A *overexpression on DA neuron differentiation of iPSC*

We next tested whether the strategy of overexpressing *LMX1A* under the neural *NESTIN* enhancer could promote appropriate DA neuron differentiation from human iPSC. For this purpose, we transduced iPSC with LV.NES.LMX1A.GFP or with control LVs. LMX1A overexpression was verified at the protein level by immunofluorescence at Stage 2 (Fig. 6a and g). Neuronal and DA neuron differentiation were evaluated at the end of Stage 3 by immunofluorescence analyses against TUJ1 and TH, respectively (Fig. 6b–e and h–k), and the maturation state of DA neurons by DAT expression (Fig. 6f and l). In addition to this, we followed by quantitative RT-PCR the expression of the pluripotency-associated gene *NANOG*, and those of the DA neuron differentiation markers *NURR1*, *EN1*, and *TH* (Fig. 6m and p). Overall, the results of these analyses were very similar to those of hESC and showed that overexpression of *LMX1A* did not significantly change the percentage of neurons differentiated from iPSC, but dramatically increased the proportion of neurons that are coaxed toward a DA neuron fate (Fig. 6q). Moreover, the presence of synaptic proteins such as synaptophysin was detected in discrete puncta that colocalized with TH immunoreactivity (Fig. 6r), suggesting the establishment of DA synaptic terminals. Finally, analyses of DA release confirmed the functionality of DA neurons differentiated from iPSC overexpressing *LMX1A* (Fig. 6s).

Discussion

One of the major bottlenecks to the development of hESC/iPSC-based strategies for modeling and treating human disease is the relative lack of efficient directed differentiation protocols for generating the specific cell type(s) relevant to the disease. In the case of PD, a variety of protocols have been described that promote the differentiation of hESC/iPSC toward DA neurons (for review, see Hwang *et al.*, 2010), but in most cases these were not appropriately patterned as A9-subtype ventral midbrain DA neurons, the relevant cell type for PD. Forcing the expression of patterning- and/or fate-associated transcription factors may help overcome this limitation, as evidenced by studies in which *Lmx1a* (Andersson *et al.*, 2006; Friling *et al.*, 2009) or a combination of *Nurr1* and *Pitx3* (Martinat *et al.*, 2006) or *Nurr1* and *Foxa2* (Lee *et al.*, 2010) was overexpressed in mouse neural precursor cells. Here, we decided to focus on LMX1A, because it was the only transcription factor the overexpression of which had been shown to clearly increase the percentage of ventral midbrain DA neurons differentiated from human neural progenitors (Friling *et al.*, 2009). In this latter work, hESC-derived neural progenitors were transduced with LVs expressing *Lmx1a* under a constitutive *PGK* promoter. Building on these data, we decided to exploit the ability of LVs to provide long-term and robust transgene expression in pluripotent stem cells and neural progenitors (Lois *et al.*, 2002; Pfeifer *et al.*, 2002; Ma *et al.*, 2003; Consiglio *et al.*, 2004), as well as the selectivity of expression in neural progenitor cells

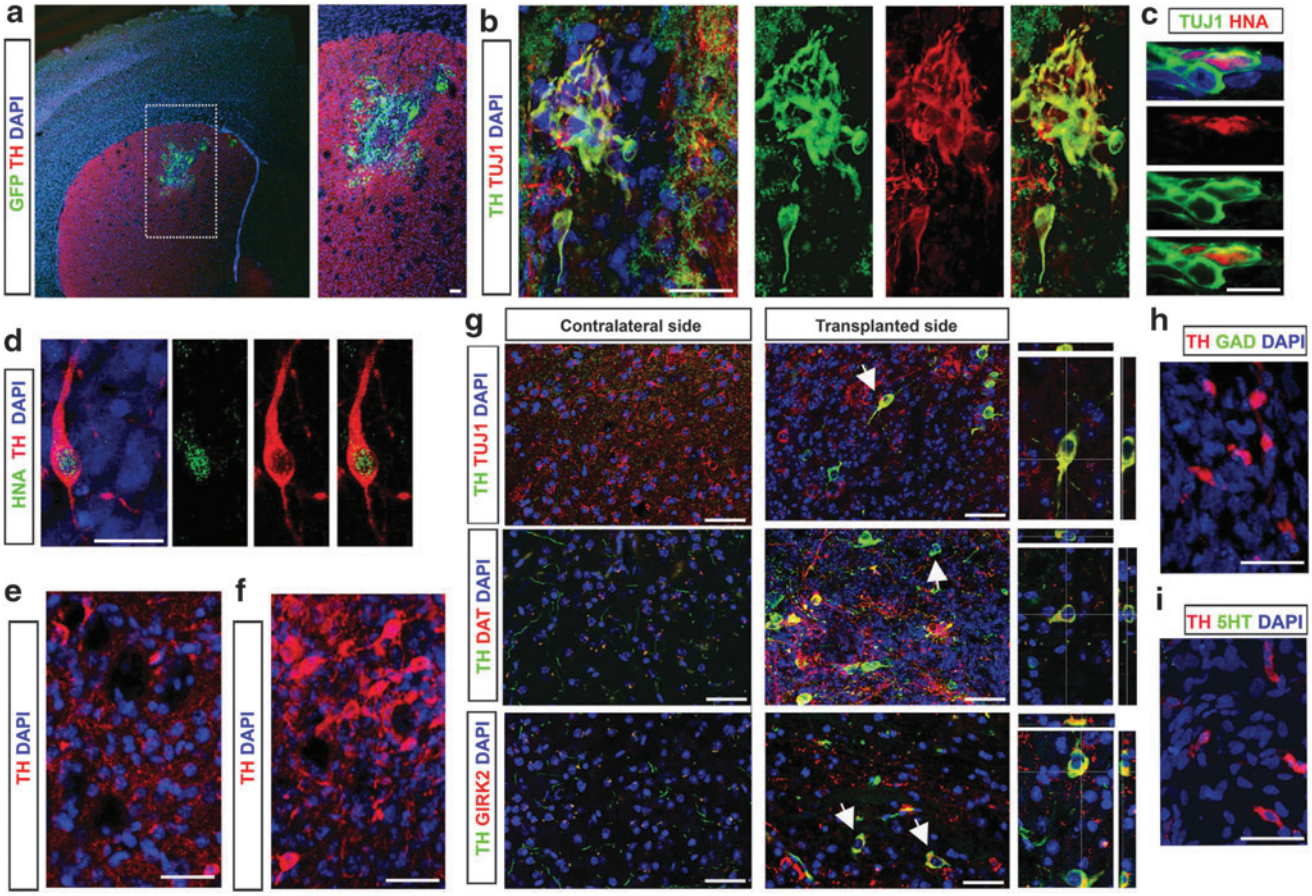

FIG. 5. Functional characterization of the DA neurons generated. **(a)** Section of the brain 1 month after transplantation of cells transduced with LV.PGK.GFP showing engraftment and survival of the infected cells. (*Inset*) Presence of GFP-positive cells in the injected area. **(b, c)** Analysis of mouse brain 4 weeks after receiving transplantation of hES-LMX1A (clone D) at Stage 3. **(b)** Grafted cells stain positive for TUJ1 and TH. **(c)** The neurons (TUJ1-positive cells) within the graft area show HNA staining, indicating their human origin. **(d–i)** Sections of mouse brains 5 months after transplantation of mock-hESC and hES-LMX1A (clone D) at Stage 3. Grafted dopaminergic cells are of human origin, as judged by HNA staining **(d)**, and survive in the host mouse brain 5 months after transplantation of mock-hESC **(e)**, and in much larger numbers after transplantation of hES-LMX1A cells **(f)**. **(g)** hES-LMX1A cells are able to differentiate toward midbrain DA neurons *in vivo* 5 months after transplantation. Immunostaning for TUJ1, TH, GIRK2, and DAT in the contralateral side shows the typical staining of dopaminergic fibers in the intact striatum. In the injected side, newly generated midbrain DA neurons that are TH-, DAT-, GIRK2-positive could be observed. **(h, i)** Absence of GABAergic neurons (GAD-positive cells; **h**) and serotonergic neurons (5-HT-positive cells; **i**) in the transplanted area. Scale bar = 50 μm.

conferred by the neural *NESTIN* enhancer (Lothian and Lendahl, 1997; Andersson *et al.*, 2006), to address whether: (1) human pluripotent stem cells can be stably engineered to express LMX1A while maintaining their characteristic self-renewal and pluripotent differentiation abilities; and (2) expression of *LMX1A* in the context of engineered hESC/iPSC is sufficient to direct the fate of differentiating neural progenitors toward ventral midbrain DA neurons of the A9 subtype.

On the first issue, our results show that clonal lines of hESC containing one or two copies of the integrated *LMX1A*-expressing LVs retain the typical features of nonmanipulated hESC, including colony morphology and growth characteristics, long-term self-renewing ability while maintaining a stable karyotype, expression of pluripotency-associated transcription factors and surface markers, *in vitro* differentiation into derivatives of the three main embryo germ layers, and teratoma formation ability (Fig. 3). This is particularly important because, even though we confirmed the specificity of expression of the neural *NESTIN* enhancer in neural progenitors (Fig. 2), there was measurable expression of transgenic *LMX1A* in undifferentiated hESC (Fig. 4a), probably owing to leakage of our system. Therefore, it is important to note that the somewhat higher levels of *LMX1A* expression in undifferentiated hES-LMX1A cells, compared with mock-hESC, do not appear to be detrimental for their maintenance as undifferentiated, pluripotent stem cells, even upon long-term passaging.

However, when induced to differentiate toward neuronal fates, hES-LMX1A cells generated significantly higher numbers of DA neurons than mock-hESC (~40% more, based on TH/TUJ1 double staining) and, more importantly, most of these DA neurons were of the ventral midbrain A9 subtype (up to 75% of them, compared with ~25% in the case of mock-hESC, based on colabeling of TH and GIRK2). Consequently, of 100 hES-LMX1A cells, we obtained >30 A9-subtype DA neurons, versus approximately seven from

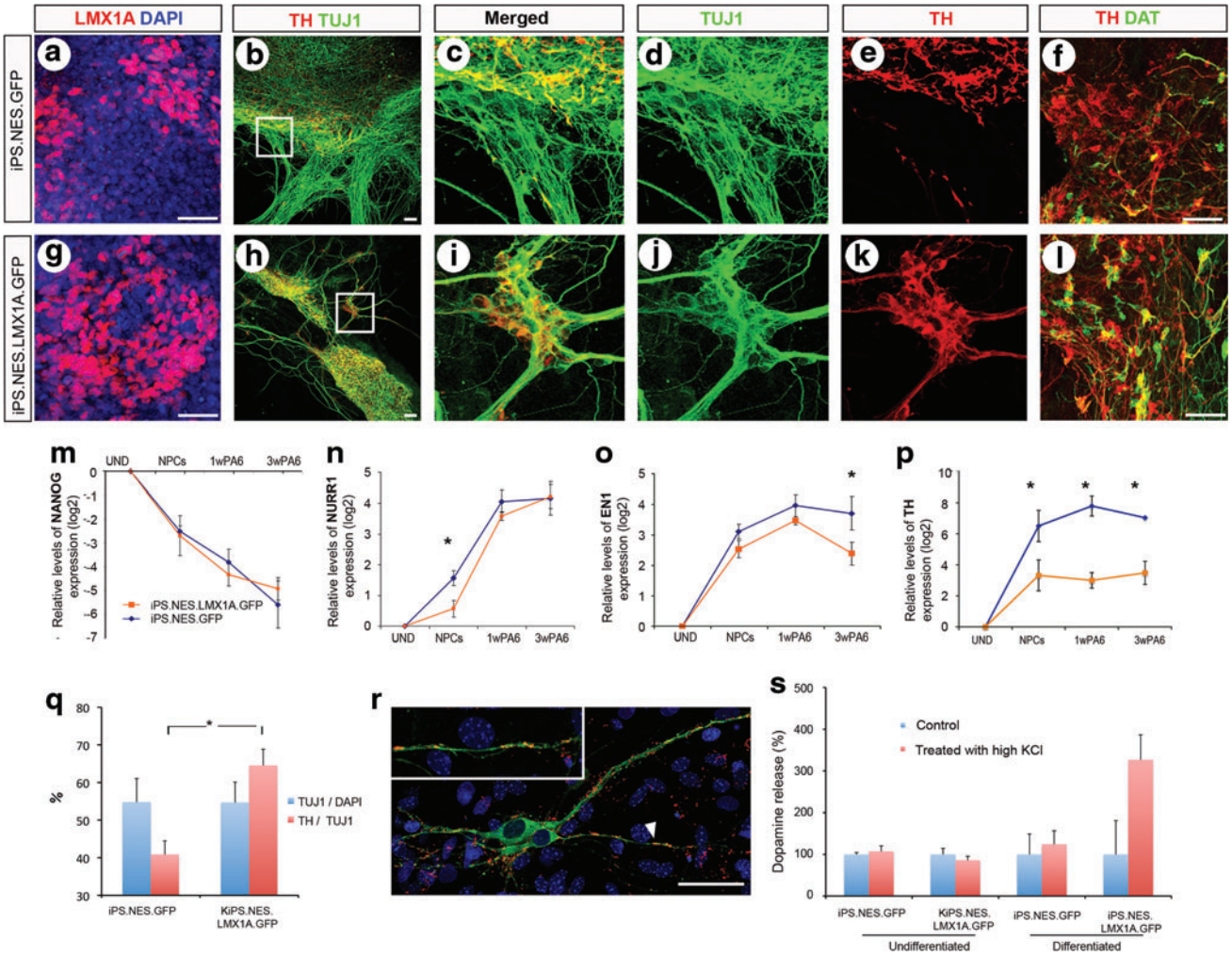

FIG. 6. LMX1A enhances generation of midbrain DA neurons in iPSC. **(a, g)** NPCs from iPS.NES.LMX1A.GFP contain more LMX1A-positive cells than those from iPS.NES.GFP. **(b, h)** Cells at Stage 3 coexpressed TUJ1 and TH. Higher magnification images **(c–e, i–k)** showed extensive presence of TH-positive cells in iPS.NES.LMX1A.GFP compared with iPS.NES.GFP. **(f, l)** TH and DAT immunocytochemistry performed at the same stage of differentiation. **(m)** qPCR analysis presenting a decrease in the expression levels of *NANOG* as the differentiation occurred in both lines. Higher levels of expression of *NURR1* **(n)** and *EN1* **(o)** are evident in iPS.NES.LMX1A.GFP than in iPS.NES.GFP. **(p)** Markedly higher expression of TH in iPS.NES.LMX1A.GFP in relation to iPS.NES.GFP. **(q)** Quantification of the neuronal and dopaminergic yield at Stage 3. The staining of TUJ1 is ~55% in both lines. Approximately 40% of the neurons are labeled with TH in iPS.NES.GFP, and this value increases to 65% in iPS.NES.LMX1A.GFP. **(r)** Immunocytochemical analysis for the presynaptic-specific marker synaptophysin (SYP, red channel) and TH (green channel); the area indicated with an arrowhead is shown in the *inset* at higher magnification. **(s)** Release of DA after treatment with high potassium concentration is found in differentiated DA neurons from iPS.NES.LMX1A.GFP. In all experiments, $n = 3$. $^*p < 0.05$. Scale bar = 50 μm. Color images available online at www.liebertonline.com/hum

mock-hESC, that is, close to a fivefold increase in the overall yield of the differentiation procedure. These differences are consistent with more differentiating cells being recruited into the ventral midbrain DA neuron lineage as transgenic *LMX1A* begins to be expressed in neural precursors, as evidenced by the increased numbers of LMX1A-positive cells in Stage 2 of differentiation.

Our results show that, under ventralizing conditions such as exposure to SHH, LMX1A is sufficient to direct the differentiation of human neural progenitors toward ventral midbrain DA neurons. This is in agreement with previous studies in the mouse, conducted by the Ericson laboratory (Andersson *et al.*, 2006; Friling *et al.*, 2009), and also in human cells (Friling *et al.*, 2009). Therefore, the reported failure of other groups to induce human DA neuron differentiation by overexpressing *LMX1A* (Roybon *et al.*, 2008; Cai *et al.*, 2009) is likely the result of inadequate levels of expression of this factor, due either to low transfection efficiency (Cai *et al.*, 2009) or to strong overexpression driven by retroviruses (Roybon *et al.*, 2008). In this regard, it is important to note that the levels of *LMX1A* expression achieved in our clonal hES-LMX1A cell lines harboring one or two LV integrations are in the same range of endogenous *LMX1A* expression levels during DA differentiation. Thus, *LMX1A* expression in hES-LMX1A cells, at its peak in mid-Stage 3, is roughly only three times higher than that of mock-hESC (Fig. 4a). Taking

into account that, as discussed above, the number of cells undergoing A9 DA neuron differentiation is about five times higher in hES-LMX1A cells than in mock-hESC, it follows that the levels of *LMX1A* expression per cell should be within the same order of magnitude in either case.

Our results also show that hES-LMX1A cells committed to DA lineages *in vitro* are able to complete differentiation to A9 ventral midbrain DA neurons upon grafting into the adult mouse brain. We transplanted differentiating cells at mid-Stage 3 (after 2 weeks of coculture with PA6 cells), because we surmised that cells at this stage of differentiation, at which they express high levels of *NURR1*, *EN1*, *ALDH1A1*, and *TH* (see Fig. 4c–f), would have become depleted of undifferentiated progenitors but were not yet fully differentiated, thus making them more likely to survive after grafting. Indeed, viable grafted cells were recovered 5 months after transplantation and shown to have completed differentiation *in situ*. Conversely, mock-hESC pretreated *in vitro* under the same conditions and transplanted into adult mouse brains differentiated very poorly *in vivo*, in agreement with previous reports that highlighted the inability of adult brain tissue to direct transplanted human neural progenitors to acquire the DA neuron fate (Ben-Hur *et al.*, 2004). Therefore, in the absence of appropriate environmental cues, transgenic *LMX1A* expression appears to maintain a ventral midbrain DA neuron differentiation program in hES-LMX1A cells.

Our strategy of LV-mediated engineering of human pluripotent stem cells to overexpress *LMX1A* in neural progenitors provides an efficient way to generate enriched populations of neurons with the characteristics of A9 ventral midbrain DA neurons. As this strategy is applicable to both hESC and iPSC, it should be suitable for modeling PD pathogenesis *in vitro*, as well as worth considering when designing future cell-therapy applications for this disease.

Acknowledgments

We thank Teresa Lopez-Rovira, Senda Jiménez, and Alberto Garcia for excellent technical assistance, José Miguel Andrés Vaquero for assistance with flow cytometry, Mercé Martí and Lola Mulero Pérez for bioimaging assistance, and Federico Gonzalez for assistance with Southern blot analyses. We are thankful to Dr. M.S. German, University of California, San Francisco Diabetes Center, for providing the Lmx1a antibody. We are also grateful to Miguel A. Valverde and José Manuel Fernández for assistance in preliminary electrophysiological studies. A.S.-D. and I.R.-P. were partially supported by predoctoral fellowships from the Spanish Ministry of Science and Education (MEC). A.C. was supported in part by the Programa Ramon y Cajal from the Spanish Ministry of Science and Innovation (MICINN). Additional support was provided by grants from MICINN (BFU2009-13277, PLE2009-0144, and ACI2010-1117 to A.R.; BFU2010-21823 to A.C.), FIS (PI061897, CP05/00294), and Fondazione Guido Berlucchi 2010 (to A.C.). The work is also part of a CIBERNED Cooperative Project (to A.C., A.R., and M.V.). Work in the laboratory of J.C.I.B. was supported by MICINN, Fundacion Cellex, Tercel, Sanofi-Aventis, and the G. Harold and Leila Y. Mathers Charitable Foundation.

Author Disclosure Statement

All authors have nothing to disclose.

References

Aasen, T., Raya, A., Barrero, M.J., *et al.* (2008). Efficient and rapid generation of induced pluripotent stem cells from human keratinocytes. Nat. Biotechnol. 26, 1276–1284.

Agarwal, S., Loh, Y.H., McLoughlin, E.M., *et al.* (2010). Telomere elongation in induced pluripotent stem cells from dyskeratosis congenita patients. Nature 426, 292–296.

Andersson, E., Tryggvason, U., Deng, Q., *et al.* (2006). Identification of intrinsic determinants of midbrain dopamine neurons. Cell 124, 393–405.

Ben-Hur, T., Idelson, M., Khaner, H., *et al.* (2004). Transplantation of human embryonic stem cell-derived neural progenitors improves behavioral deficit in Parkinsonian rats. Stem Cells 22, 1246–1255.

Cai, J., Donaldson, A., Yang, M., *et al.* (2009). The role of Lmx1a in the differentiation of human embryonic stem cells into midbrain dopamine neurons in culture and after transplantation into a Parkinson's disease model. Stem Cells 27, 220–229.

Consiglio, A., Gritti, A., Dolcetta, D., *et al.* (2004). Robust in vivo gene transfer into adult mammalian neural stem cells by lentiviral vectors. Proc. Natl. Acad. Sci. U.S.A. 101, 14835–14840.

Dimos, J.T., Rodolfa, K.T., Niakan, K.K., *et al.* (2008). Induced pluripotent stem cells generated from patients with ALS can be differentiated into motor neurons. Science 321, 1218–1221.

Ebert, A.D., Yu, J., Rose, F.F., Jr., *et al.* (2009). Induced pluripotent stem cells from a spinal muscular atrophy patient. Nature 457, 277–280.

Friling, S., Andersson, E., Thompson, L.H., *et al.* (2009). Efficient production of mesencephalic dopamine neurons by Lmx1a expression in embryonic stem cells. Proc. Natl. Acad. Sci. U.S.A. 106, 7613–7618.

Hanna, J., Wernig, M., Markoulaki, S., *et al.* (2007). Treatment of sickle cell anemia mouse model with iPS cells generated from autologous skin. Science 318, 1920–1923.

Hwang, D.Y., Kim, D.S., and Kim, D.W. (2010). Human ES and iPS cells as cell sources for the treatment of Parkinson's disease: current state and problems. J. Cell. Biochem. 109, 292–301.

Inanobe, A., Yoshimoto, Y., Horio, Y., *et al.* (1999). Characterization of G-protein-gated K^+ channels composed of Kir3.2 subunits in dopaminergic neurons of the substantia nigra. J. Neurosci. 19, 1006–1017.

Isacson, O., Bjorklund, L.M., and Schumacher, J.M. (2003). Toward full restoration of synaptic and terminal function of the dopaminergic system in Parkinson's disease by stem cells. Ann. Neurol. 53(Suppl. 3), S135–S146; discussion S146–S138.

Kawasaki, H., Suemori, H., Mizuseki, K., *et al.* (2002). Generation of dopaminergic neurons and pigmented epithelia from primate ES cells by stromal cell-derived inducing activity. Proc. Natl. Acad. Sci. U.S.A. 99, 1580–1585.

Lee, H.S., Bae, E.J., Yi, S.H., *et al.* (2010). Foxa2 and Nurr1 synergistically yield A9 nigral dopamine neurons exhibiting improved differentiation, function, and cell survival. Stem Cells 28, 501–512.

Lee, S.H., Lumelsky, N., Studer, L., *et al.* (2000). Efficient generation of midbrain and hindbrain neurons from mouse embryonic stem cells. Nat. Biotechnol. 18, 675–679.

Lie, D.C., Colamarino, S.A., Song, H.J., *et al.* (2005). Wnt signalling regulates adult hippocampal neurogenesis. Nature 437, 1370–1375.

Lindvall, O., and Björklund, A. (2004). Cell therapy in Parkinson's disease. NeuroRx 1, 382–393.

Lois, C., Hong, E.J., Pease, S., *et al.* (2002). Germline transmission and tissue-specific expression of transgenes delivered by lentiviral vectors. Science 295, 868–872.

Lothian, C., and Lendahl, U. (1997). An evolutionarily conserved region in the second intron of the human nestin gene directs gene expression to CNS progenitor cells and to early neural crest cells. Eur. J. Neurosci. 9, 452–462.

Lowry, W.E., Richter, L., Yachechko, R., *et al.* (2008). Generation of human induced pluripotent stem cells from dermal fibroblasts. Proc. Natl. Acad. Sci. U.S.A. 105, 2883–2888.

Ma, Y., Ramezani, A., Lewis, R., *et al.* (2003). High-level sustained transgene expression in human embryonic stem cells using lentiviral vectors. Stem Cells 21, 111–117.

Marsden, C.D. (1990). Parkinson's disease. Lancet 335, 948–952.

Martinat, C., Bacci, J.J., Leete, T., *et al.* (2006). Cooperative transcription activation by Nurr1 and Pitx3 induces embryonic stem cell maturation to the midbrain dopamine neuron phenotype. Proc. Natl. Acad. Sci. U.S.A. 103, 2874–2879.

Mendez, I., Sanchez-Pernaute, R., Cooper, O., *et al.* (2005). Cell type analysis of functional fetal dopamine cell suspension transplants in the striatum and substantia nigra of patients with Parkinson's disease. Brain 128, 1498–1510.

Morales, R., Riss, M., Wang, L., *et al.* (2008). Integrating multiunit electrophysiology and plastic culture dishes for network neuroscience. Lab Chip 8, 1896–1905.

Morizane, A., Li, J.Y., and Brundin, P. (2008). From bench to bed: the potential of stem cells for the treatment of Parkinson's disease. Cell Tissue Res. 331, 323–336.

Naldini, L., Blomer, U., Gallay, P., *et al.* (1996). In vivo gene delivery and stable transduction of nondividing cells by a lentiviral vector. Science 272, 263–267.

Nat, R., Nilbratt, M., Narkilahti, S., *et al.* (2007). Neurogenic neuroepithelial and radial glial cells generated from six human embryonic stem cell lines in serum-free suspension and adherent cultures. Glia 55, 385–399.

Park, I.H., Arora, N., Huo, H., *et al.* (2008a). Disease-specific induced pluripotent stem cells. Cell 134, 877–886.

Park, I.H., Zhao, R., West, J.A., *et al.* (2008b). Reprogramming of human somatic cells to pluripotency with defined factors. Nature 451, 141–146.

Pfeifer, A., Ikawa, M., Dayn, Y., and Verma, I.M. (2002). Transgenesis by lentiviral vectors: lack of gene silencing in mammalian embryonic stem cells and preimplantation embryos. Proc. Natl. Acad. Sci. U.S.A. 99, 2140–2145.

Raya, A., Rodriguez-Piza, I., Aran, B., *et al.* (2008). Generation of cardiomyocytes from new human embryonic stem cell lines derived from poor-quality blastocysts. Cold Spring Harb. Symp. Quant. Biol. 73, 127–135.

Raya, A., Rodriguez-Piza, I., Guenechea, G., *et al.* (2009). Disease-corrected haematopoietic progenitors from Fanconi anaemia induced pluripotent stem cells. Nature 460, 53–59.

Raya, A., Rodriguez-Piza, I., Navarro, S., *et al.* (2010). A protocol describing the genetic correction of somatic human cells and subsequent generation of iPS cells. Nat. Protoc. 5, 647–660.

Roy, N.S., Cleren, C., Singh, S.K., *et al.* (2006). Functional engraftment of human ES cell-derived dopaminergic neurons enriched by coculture with telomerase-immortalized midbrain astrocytes. Nat. Med. 12, 1259–1268.

Roybon, L., Hjalt, T., Christophersen, N.S., *et al.* (2008). Effects on differentiation of embryonic ventral midbrain progenitors by Lmx1a, Msx1, Ngn2, and Pitx3. J. Neurosci. 28, 3644–3656.

Smidt, M.P., and Burbach, J.P. (2007). How to make a mesodiencephalic dopaminergic neuron. Nat. Rev. Neurosci. 8, 21–32.

Soldner, F., Hockemeyer, D., Beard, C., *et al.* (2009). Parkinson's disease patient-derived induced pluripotent stem cells free of viral reprogramming factors. Cell 136, 964–977.

Takahashi, K., Tanabe, K., Ohnuki, M., *et al.* (2007). Induction of pluripotent stem cells from adult human fibroblasts by defined factors. Cell 131, 861–872.

Thomson, J.A., Itskovitz-Eldor, J., Shapiro, S.S., *et al.* (1998). Embryonic stem cell lines derived from human blastocysts. Science 282, 1145–1147.

Trzaska, K.A., Kuzhikandathil, E.V., and Rameshwar, P. (2007). Specification of a dopaminergic phenotype from adult human mesenchymal stem cells. Stem Cells 25, 2797–2808.

Wernig, M., Zhao, J.P., Pruszak, J., *et al.* (2008). Neurons derived from reprogrammed fibroblasts functionally integrate into the fetal brain and improve symptoms of rats with Parkinson's disease. Proc. Natl. Acad. Sci. U.S.A. 105, 5856–5861.

Ying, Q.L., Stavridis, M., Griffiths, D., *et al.* (2003). Conversion of embryonic stem cells into neuroectodermal precursors in adherent monoculture. Nat. Biotechnol. 21, 183–186.

Yu, J., Vodyanik, M.A., Smuga-Otto, K., *et al.* (2007). Induced pluripotent stem cell lines derived from human somatic cells. Science 318, 1917–1920.

Address correspondence to:
Dr. A. Consiglio
The Institute of Biomedicine of the University of Barcelona (IBUB)
Parc Cientific de Barcelona
Baldiri Reixac 15-21
08028 Barcelona
Spain

E-mail: aconsiglio@pcb.ub.es

Dr. J.C. Izpisua Belmonte
Center of Regenerative Medicine in Barcelona (CMRB)
Dr. Aiguader, 88
08003 Barcelona
Spain

E-mail: belmonte@salk.edu

Received for publication April 4, 2011;
accepted after revision August 29, 2011.

Published online: August 30, 2011.